Analysis of OCTA Features of the Retina and DTI Features of the Visual Pathway in Patients with Pituitary Adenoma

Zhi Tan
Guangzhou Medical University

Zhihui Liao
Guangzhou Medical University

Shuying Peng
Guangzhou Medical University

Xiujuan Wen
Guangzhou Medical University

Wei Mo
Guangzhou Medical University

Keqi Xiao
Guangzhou Medical University

Xiaoying Lai
Guangzhou Medical University

Yanhua Pang（✉ 1049371818@qq.com ）
Guangzhou Medical University

Additional Declarations: No competing interests reported.

Abstract

Purpose

The objective of this research is to investigate the ocular neural pathway in individuals affected by pituitary adenoma (PA), by combining two distinct methods: diffusion tensor imaging (DTI) and optical coherence tomography angiography (OCTA). The relationship between retinal blood flow density and neural fiber conduction function in these patients is explored.

Methods

The case group comprised 24 individuals who had been recently identified and pathologically verified as suffering from PA. A control group was assembled, consisting of 24 subjects who were aligned with the case group in terms of age and gender. All participants underwent OCTA, optical coherence tomography (OCT), and DTI examinations. Differences in the optic disc, macular OCTA parameters, OCT parameters, and DTI parameters between the two groups were compared, and correlations between these parameters were discussed.

Results

DTI parameters: In the case group, the optic nerve, optic chiasm, optic tract, and optic radiation showed a decline in their fractional anisotropy (FA) values when juxtaposed with the control group. Concurrently, the apparent diffusion coefficient (ADC) values for the optic nerve and optic radiation escalated in comparison to the control group. Parameters of OCTA: In the region of the macula, the density of blood flow across all layers, barring the deep capillary plexus (DCP), was found to be lesser in the subject group when contrasted with the reference group. There was a notable decline in the blood flow density in the radial peripapillary capillaries plexus (RPCP) and the superficial vascular complex (SVC) as well when set against the reference group. Correlation: A statistically significant correlation existed between the blood flow density of all layers of the macular area and the DTI parameters of the optic radiation. Importantly, strong associations were found between the superficial vascular network (SVN) in the macular area and the ADC measurement of the optic nerve, the FA measurement of the optic tract, and the ADC measurement of the optic radiation. This suggests that these values might serve as biomarkers for assessing neural fiber conduction function in the visual pathway.

Conclusion

OCTA can assess retinal blood flow density in PA patients, while DTI quantifies neural fiber conduction function. The combination of these techniques offers a novel approach for studying visual pathway injury in PA.

1 Introduction

Pituitary adenomas (PA) are commonly observed tumors in the cranial region. Due to their anatomical proximity to the optic chiasm, an enlarging adenoma progressively contacts and compresses the chiasm, resulting in clinical manifestations such as diminished visual acuity and impaired visual field. Numerous investigations, including our own prior work, have noted that for individuals with pseudoxanthoma elasticum (PA), the optical coherence

tomography (OCT) imaging of the optic nerve and macular area consistently shows a reduction in thickness, either in particular segments or more broadly, in the Circumpapillary retinal nerve fiber layer (CP-RNFL) and the macular ganglion cell complex (GCC) layer [1−3]. A recent advancement, optical coherence tomography angiography (OCTA), which is a non-intrusive method derived from OCT, allows for the quantitative assessment of vascular density in different retina layers around the optic disc and in the macular area. It provides an objective quantification of retinal microcirculation and has been extensively employed in optic nerve and retinal disease studies [4−6]. Recent OCTA-based studies have shown that the optic nerve and macular region vascular density in PA patients is decreased compared to controls, yet the precise underlying mechanism remains elusive [7−9]. Moreover, the correlation between changes in vascular density and neural conduction functionality remains uncertain. Against this backdrop, we introduced diffusion tensor imaging (DTI) into our research.

DTI, a type of functional magnetic resonance imaging, stands as the sole non-invasive method to quantitatively investigate white matter tracts in living human brain tissue, facilitating the assessment of neural fiber conduction functionality. The primary parameters include: 1. Fractional anisotropy (FA), which reflects the degree of directional diffusion of water molecules within white matter fibers. Under ideal conditions, as water molecules undergo Brownian motion, they diffuse along the longitudinal axis of neural fibers, rendering an FA value of 1. If water molecules diffuse randomly, the FA value is 0. Under normal circumstances, FA values range between 0 and 1; however, pathological conditions often lead to decreased FA values. 2. The apparent diffusion coefficient (ADC) or mean diffusivity (MD) measures the average movement of water molecules without considering fiber directionality and is used to gauge the diffusion capability and speed of water within tissues [10]. Acute brain tissue abnormalities often present with decreased ADC values, whereas sub-acute and chronic changes often show elevated ADC values. Presently, DTI has been integrated into studies across various brain-related conditions [11−13] and has been gradually introduced into the research of visual pathways in PA, including our prior investigations [14−15].

In our initial research, we evaluated OCT parameters of the optic disc and macular area in pseudoxanthoma elasticum (PA) patients. This assessment encompassed measurements of both the Circumpapillary retinal nerve fiber layer (CP-RNFL) thickness and the Ganglion Cell Complex (GCC) thickness. We also explored the characteristics and correlation of these parameters with visual pathway DTI metrics. In this study, our primary objective was to delve deeper into the variations in retinal vascular density in PA patients and to discern its relationship with neural conduction functions. We assessed OCTA parameters of the optic disc and macular region, along with DTI metrics of the optic nerve, optic chiasm, optic tract, and optic radiation, and conducted a correlation analysis. To the best of our knowledge, this is the pioneering research globally that combines OCTA and DTI to study the visual pathway damage in PA patients.

2 Objective and Methodology

2.1 Objective

This study is a prospective clinical case-control investigation. We included 24 patients diagnosed with pituitary adenoma (PA) through magnetic resonance imaging and post-operative pathological examination, who were admitted to the Neurosurgery Department of the Affiliated Hospital of Guangdong Medical University between September 2021 and March 2023, as the PA group. Another 24 individuals from the general population served as the control group. Each participant was subjected to a series of assessments, including determining the finest

vision correction (BCVA), visual field testing, optic disc analysis, macular OCT, and OCTA tests, along with visual pathway DTI assessment. This research adhered to the guidelines established by the Helsinki Declaration, and all involved parties provided their consent by signing the necessary documents. All research-related data received ethical committee approval (No. PJ2020-006, VJ2020-006-03, KT2022-038).

Criteria for Inclusion and Exclusion for PA Group:

1. Brain MRI scans, both plain and enhanced, suggesting pituitary adenoma.
2. The complete removal of the adenoma through endoscopic nasal transsphenoidal surgery, with pathology confirming it as a pituitary adenoma.
3. Age between 18 and 65 years.
4. The non-invasive assessment of intraocular tension indicated a reading of ≤ 21 mmHg (1 mmHg equals 0.133 kPa).
5. There was no preceding incidence of diseases affecting the skull, injury, or surgical procedures performed on the cranium. Additionally, there was no documented instance of eye injury, glaucoma, maladies affecting the optic nerve or retina, or any past surgeries on the intraocular region.
6. Refractive errors were less than < ± 6.0D (spherical) and < 3.00D (cylindrical).
7. Clear OCT images and good quality DTI imaging.

Criteria for Inclusion and Exclusion of the Control Group:

1. The intraocular pressure, measured non-invasively, was less than or equal to 21 mmHg.
2. Either the visual acuity or the corrected visual acuity was greater than or equal to 0.8, and the refractive errors were less than 6.0D (spherical) and 3.00D (cylindrical).
3. Absence of a past record of diseases inside the skull, any injuries, or operations on the skull.
4. Absence of ocular trauma, glaucoma, optic nerve or retinal diseases, and any prior intraocular surgeries.
5. Age and gender matching with the PA group.
6. Clear OCT images and good quality DTI imaging.

2.2 Visual Field Examination

Prior to surgery for the PA group and following the correction of refractive errors in the control group, a visual field assessment was carried out using the Kowa AP7000 precision visual field analyzer from Kowa, Japan. A pair of trustworthy assessments of the visual field were carried out, concentrating on the central 30 degrees. In instances where fixation was interrupted, or when the rate of false-negative or false-positive errors surpassed 20%, the evaluation was deemed as untrustworthy. The Mean Defect (MD) metric was utilized to assess the comprehensive impairment of the visual field.

2.3 MRI Examination of the Tumor:

In the PA group, all patients underwent preoperative plain and contrast-enhanced head MRI scans using the Discovery MR750 3.0T scanner from GE, USA, to assess tumor dimensions. Following the guidelines provided in reference 15, the tumor's maximum length, width, and height were measured and documented. Additionally, the thickness of the optic chiasm was recorded. Each measurement was repeated three times, and the average value was documented.

2.4 DTI Examination and Image Post-processing

Each participant underwent T1-weighted imaging (T1WI) and diffusion tensor imaging (DTI) utilizing the GE 3.0T Optima MR360 imaging device, which includes a 16-channel head phased array coil. Scan parameters: For T1WI, the Ax 3D BRAVO sequence was used with scanning parameters of TR/TE 12.3/5.1ms, matrix 256×256, FOV 240mm×240mm, slice thickness 1.4mm, interval 0mm, and NEX of 1. In the case of DTI, we employed a single-shot stimulated DW-SE-EPI sequence with the following parameters: TR/TE of 9000/100.1ms, matrix size of 128×128, field of view (FOV) measuring 240mm×240mm, single acquisition, 25 diffusion sensitivity gradient directions, a b-value of 1000s/mm², and a slice thickness and spacing of 2/0mm. The orientation of the scan was axial, facilitating the acquisition of tensor FA images and ADC images, color-coded respectively. During the preprocessing of DTI data, the following color assignments were made: anteroposterior (green), left-right (red), and superior-inferior (blue). Comprehensive measurements and analyses of the optic nerve, optic tract, and optic radiation were carried out in both subject groups, encompassing the anterior, middle, and posterior segments, as well as the left, middle, and right sections of the optic chiasm. These evaluations were conducted using the GE 3.0T MRI machine's integrated software (ADW 4.2 function tool). To achieve the most accurate depiction of the bilateral optic tracts, and optic radiation, bilateral optic nerves, optic chiasm, three separate regions of interest (ROIs) were chosen, and the FA and ADC values within these regions were recorded. The ROIs were identified and measured based on established neuroanatomical definitions and pertinent literature, with the sizes of the ROIs varying between 8 and 12 mm^2. A single physician consistently conducted all measurements, and the mean FA and ADC values for the optic nerve, optic chiasm, optic tract, and optic radiation were determined from the measurements obtained from the three separate ROIs. (Refer to Figs. 1 and 2).

2.5 OCT and OCTA Examination

Both OCT and OCTA were performed by the same experienced ophthalmologist using the OCT device (Heidelberg Engineering Spectralis, Germany). For all patients, measurements were taken of the thickness of the circumpapillary retinal nerve fiber layer (CP-RNFL), the ganglion cell complex (GCC), the inner plexiform layer (IPL) in the macula, and the macular ganglion cell layer (GCL). Scans utilized a center wavelength of 870nm swept-source laser with a speed of 8.8 frames per second and "High Speed" resolution. The optic disc region used the standard international diameter of 3.45mm ring pattern (768A-scans) centered on the optic disc to capture RNFL thickness. The macular region selected a volume scan mode, centered on the fovea, with a scanning range of 8.8mm×8.8mm (31 lines, spaced 240µm, 768A-scans). Built-in software was used for image analysis, measuring the thickness of different quadrants and layers of the retina in the macular region. The total thickness of RNFL, GCL, and IPL was designated as GCC. With "High Res" resolution (5.7um/pixel), scans centered on the fovea covered a 3mm×3mm area (spaced 6µm, 512A-scans) for OCTA to acquire images at different layers of vessel density (VD) in the macular area. When centered on the optic disc, the range was 6mm×6mm for OCTA to capture VD images next to the optic disc. The VD of the optic disc included radial peripapillary capillaries plexus (RPCP), superficial vascular complex (SVC), superficial vascular plexus (SVP), intermediate capillary plexus (ICP), deep vascular complex (DVC), and deep capillary plexus (DCP). The macular region's VD included SVC, SVP, ICP, DVC, and DCP.

2.6 Image Processing and Analysis Methods

Raw VD images of the optic disc and macular region for SVC, DVC, SVP, ICP, and DCP were exported from the OCTA database. Using Image J software (version 1.53), images were processed in 8-bit grayscale format and

thresholded. Images were then binarized to clearly differentiate microvessels. Subsequently, VD at various layers was calculated, with VD defined as the percentage of the image area occupied by vessels (Refer to Figs. 3 and 4).

2.7 Data Evaluation

The analysis of the data was performed utilizing the SPSS 24.0 software. Continuous variables that satisfied the normality requirements of the Shapiro-Wilk test were represented using mean and standard deviation (± s). Comparisons between different groups were conducted using the independent samples t-test for continuous variables, and the chi-square test for categorical data. Pearson's r was used to assess the correlation between two continuous variables that followed a normal distribution. In cases where the data was not normally distributed, the Spearman's rank correlation was applied. A P-value less than 0.05 was deemed to indicate a statistically significant difference.

3 Results

3.1 General Information

The group in question consisted of 15 men and 9 women, whose average age was approximately 47.958 ± 15.638 years. Among the 24 patients with PA, there were 2 with adrenocorticotropic adenomas, 2 with gonadotropic adenomas, 2 with prolactin cell tumors, 1 with growth hormone cell tumor, and 1 with a mixed growth hormone cell and prolactin cell tumor. The rest had non-secreting adenomas. A group of 24 healthy volunteers, who gave informed consent, served as the control group, consisting of 12 males and 12 females with an average age of 50.291 ± 16.619 years. No notable difference in age and gender was observed between the two groups. There was a statistical difference in the best-corrected visual acuity (BCVA) and visual field (mean defect, MD) values when comparing the two patient groups with the normal control group (Table 1).

3.2 Comparison of DTI Parameters of Visual Pathway Between Case and Control Groups

The FA measures of the optic nerve, chiasm, tract, and radiation were found to be lower in the case group when juxtaposed with the control group. Additionally, the ADC values pertaining to the optic nerve and optic radiation were observed to be elevated in the case group relative to the control group, as indicated in Table 2.

3.2 Comparison of OCTA Parameters Between Case and Control Groups

Within the macular region, the density of blood flow in all layers, barring the DCP layer, was notably less than in the control group, a difference that was statistically significant. Yet, it was noted that the density of blood flow in the macular region's DCP layer was still less than that of the control group. Additionally, the RPCP and SVC in proximity to the optic disc were also inferior to the measurements in the control group (See Table 3).

3.4 Comparison of OCT Parameters Between Case and Control Groups (See Table 4)

In the case group, the average, temporal, and inferior CP-RNFL were thinner than in the control group. In the macular area, the superior inner ring GCL layer, IPL layer, nasal side, and superior GCC layer were thinner than in the control group (See Table 4).

3.5 Association Among OCTA Metrics, OCT Metrics, and DTI Metrics of Visual Route (Refer to Table 5)

1. The SVP of the macular region exhibited the most robust association with the ADC value of the optic nerve, FA value of the optic tract, and ADC value of the optic radiation, evidenced by r values of -0.478, 0.557, and − 0.640, respectively. P-values were 0.018, 0.005, and 0.001. This suggests that the SVP of the macular area can effectively reflect the neural fiber conduction function of the visual pathway.

2. The SVP in the macular area exhibited the most pronounced positive correlation with the thickness of the inferior inner ring GCL, with an r value of 0.656 and P = 0.001. Similarly, the optic disc RPCP showed a significant positive association with the thickness of the inferior CP-RNFL, registering an r value of 0.642 and P = 0.001.

3. Each layer's blood flow density in the macular region demonstrated significant correlations with the function of the optic radiation.

3.6 Correlation Between OCTA Parameters, BCVA, MD, and Tumor Diameter

The blood flow density of the macular vessel layers DCP, DVC, and ICP had a statistically significant negative correlation with LogMAR BCVA, with r values of -0.324, -0.349, and − 0.316, respectively. P-values were 0.025, 0.015, and 0.029. The density of the SVC and RPCP layers of the optic disc had a statistically significant negative correlation with LogMAR BCVA, with r values of -0.414 and − 0.494, respectively. P-values were 0.003 and 0.000. There was no statistical correlation between the blood vessel density of the optic disc and macular area and the MD value of the visual field.

The SVP of the macular area and RPCP near the optic disc had a statistically significant negative correlation with tumor height, with r values of -0.387 and − 0.320, respectively. P-values were 0.005 and 0.021. The SVP of the macular area had a statistically significant negative correlation with the height of the tumor above the saddle, with r=-0.301 and P = 0.030.

4 Discussion

Traditional MRI only provides purely anatomical data and does not offer any information about neural fiber conduction functionality. DTI, a specialized form of diffusion-weighted MRI, has made notable strides in neuroscience. Previous studies have found that after tumor removal and the reconstruction of white matter fibers, the FA value increases, and the MD value decreases [18]. Recent research indicates that an MD value under 0.0021 and an FA value over 0.1689 can forecast favorable postoperative visual recovery outcomes [10]. In the research conducted, it was found that the FA values of the optic pathway in the group of patients were inferior when contrasted with the control group, whereas the ADC values were superior. This further confirms the conclusion that PA patients have abnormal neural fiber conduction.

Given the shared embryological origin of the eyes and the central nervous system, they are anatomically interconnected. Lima Rebouças and colleagues hypothesize that since the GCL-IPL and GCC layers are mainly composed of the bodies of ganglion cells, they reflect the thickness of the cerebral cortex and gray matter [19]. In contrast, CP-RNFL primarily consists of the axons of retinal ganglion cells, mainly reflecting the volume and microscopic changes in white matter. Whole-brain analysis has shown that a thicker CP-RNFL, GC-IPL, and GCC correspond with higher white matter microstructural integrity. Ito, Y identified a correlation between the thickness of

the macular GCC layer, GCL, and dementia, implying that retinal structure can serve as an indicator of brain health [20]. There are many studies currently using OCT to measure the thickness of the optic disc and macular layers. Our results are consistent with previous findings, showing quadrant-specific thinning of CP-RNFL and the macular region GCL, IPL, and GCC. Combined with DTI results, this indicates that PA patients may have both gray and white matter structural and functional impairments [1–3].

Another anatomical retinal marker is retinal blood flow density. Our findings have similarities and differences from previous research. Previous studies have found reduced RPCP and superficial macular capillary plexus density in PA patients [21–22]. This reduction is speculated to result from tumor growth compressing the optic chiasm, causing axoplasmic flow obstruction and reduced blood supply, leading to neural atrophy and ganglion cell death, which ultimately manifests as retinal vasoconstriction [23]. Our study identified reduced blood flow density in both the optic disc RPCP and all layers of the macular region, which aligns with the results of Gilda Cennamo and others [22]. We understand that the visual conduction pathway includes four tiers of neurons. Bipolar cells in the nuclear layer represent the second tier, and ganglion cells represent the third. The retina within the nuclear layer is supplied by the central artery, wherein the RPCP originates from the small arteries around the optic disc and extends radially from the optic disc. This supplies blood and nutrients to the ganglion cells. After the atrophy of ganglion cells, the corresponding RPCP density reduces.

For the first time, our research delves into the association between retinal blood flow density and the functionality of neural fibers within the visual pathway. We found that the blood flow density of all macular layers positively correlates with radiative FA values and negatively with ADC values, indicating that the impairment of radiative neural fiber conduction function is related to reduced macular blood flow density. The lateral geniculate body is the fourth tier of the visual conduction pathway, with radiations made up of its axons responsible for transmitting visual information to the primary visual cortex. Previous research and our preliminary studies confirm that in addition to retrograde degeneration after chiasmal compression, anterograde degeneration also occurs [25]. This forward degeneration is evident in DTI as a reduction in radial FA values and an increase in ADC values. Meanwhile, we observed the strongest correlation between macular region SVP density and optic nerve ADC value, optic tract FA value, and radiative ADC value, suggesting that the macular region SVP could serve as an indicator for evaluating the function of the visual pathway, particularly reflecting the radiative neural conduction function. However, further studies with larger samples are required to confirm this finding.

Lastly, our study found that the density of macular SVP and peripapillary RPCP negatively correlates with tumor height. We speculate that tumors with a larger vertical diameter tend to compress the optic chiasm, causing retrograde degeneration, which then reduces retinal blood flow density. Nonetheless, the correlation between the density of blood flow in the retina and the diameter of the tumor is still a subject of debate. For example, a study by Guangxin Wang et al. did not observe any association between the density of blood flow around the optic disc and the diameter of the tumor. Conversely, Xuqian Wang et al. discovered a notable association, which aligns with the results of our research [28].

Limitations of our research include the limited number of patients studied, preventing subgroup analysis, including studies on tumors compressing the optic chiasm to varying degrees. Our study is cross-sectional and does not compare the pre- and post-treatment visual pathway DTI and retinal OCTA characteristics in PA patients. To gain a more comprehensive understanding of visual pathway damage in PA patients, additional long-term studies are warranted.

References

1. Santorini, M, Ferreira De Moura, T, Barraud, S, et al. Comparative Evaluation of Two SD-OCT Macular Parameters (GCC, GCL) and RNFL in Chiasmal Compression. Eye Brain. 2022; 14 35-48.

2. Xia, L, Wenhui, J, Xiaowen, Y, et al. Predictive value of macular ganglion cell-inner plexiform layer thickness in visual field defect of pituitary adenoma patients: a case-control study. PITUITARY. 2022; 25 (4): 667-672.

3. Menon, S, Nair, S, Kodnani, A, et al. Retinal nerve fiber layer thickness and its correlation with visual symptoms and radiological features in pituitary macroadenoma. J NEUROSCI RURAL PRA. 2022; 14 (1): 41-47.

4. Shao, Y, Mao, J, Fang, Y, et al. The Characteristic of Optical Coherence Tomography Angiography and Retinal Arteries Angle in Familial Exudative Vitreoretinopathy with Inner Retinal Layer Persistence. CURR EYE RES. 2023; 48 (9): 850-856.

5. Huang, Y, Yuan, Y, Seth, I, et al. Optic Nerve Head Capillary Network Quantified by Optical Coherence Tomography Angiography and Decline of Renal Function in Type 2 Diabetes: A Three-Year Prospective Study. AM J OPHTHALMOL. 2023; 253 96-105.

6. Zhang, L, Zhuang, C, Wang, Y, et al. Clinical Observation of Macular Superficial Capillary Plexus and Ganglion Cell Complex in Patients with Parkinson's Disease. OPHTHAL RES. 2023.

7. Wei, P, Falardeau, J, Chen, A, et al. Optical coherence tomographic angiography detects retinal vascular changes associated with pituitary adenoma. Am J Ophthalmol Case Rep. 2022; 28 101711.

8. Akdogan, M, Dogan, M, Beysel, S, et al. Optical coherence tomography angiography characteristics of the retinal and optic disc morphology in prolactinoma. MICROVASC RES. 2022; 144 104424.

9. Tang, Y, Liang, X, Xu, J, et al. The Value of Optical Coherence Tomography Angiography in Pituitary Adenomas. J INTEGR NEUROSCI. 2022; 21 (5): 142.

10. Mohamadzadeh, O, Sadrehosseini, SM, Tabari, A, et al. Can Preoperative Diffusion Tensor Imaging Tractography Predict the Visual Outcomes of Patients with Pituitary Macroadenomas? A Prospective Pilot Study. WORLD NEUROSURG. 2023; 172 e326-e334.

11. Videtta, G, Squarcina, L, Rossetti, MG, et al. White matter modifications of corpus callosum in bipolar disorder: A DTI tractography review. J AFFECT DISORDERS. 2023; 338 220-227.

12. Ornello, R, Bruno, F, Frattale, I, et al. White matter hyperintensities in migraine are not mediated by a dysfunction of the glymphatic system-A diffusion tensor imaging magnetic resonance imaging study. HEADACHE. 2023; doi: 10.1111/head.14607.

13. Li, MZ, Zhang, L, Shi, ZY, et al. Magnetic resonance imaging detects cerebral gray and white matter injury correlated with cognitive impairments in diabetic db/db mice. BEHAV BRAIN RES. 2023; 451 114510.

14. Rutland JW, Padormo F, Yim CK, et al. Quantitative assessment of secondary white matter injury in the visual pathway by pituitary adenomas: a multimodal study at 7-Tesla MRI. J Neurosurg.2019;132:333-342.

15. Pang, Y, Tan, Z, Chen, X, et al. Evaluation of preoperative visual pathway impairment in patients with non-functioning pituitary adenoma using diffusion tensor imaging coupled with optical coherence tomography. Front Neurosci. 2023; 17 1057781.

16. Li M, Ke M, Song Y, et al. Diagnostic utility of central damage determination in glaucoma by magnetic resonance imaging: An observational study[J]. Exp Ther Med.2019;17(3) :1891-1895.

17. Al-Sheikh, M, Ghasemi Falavarjani, K, Akil, H, et al. Impact of image quality on OCT angiography based quantitative measurements. Int J Retina Vitreous. 2017; 3 13.

18. Anik I, Anik Y, Cabuk B, et al. Visual outcome of an endoscopic endonasal transsphenoidal approach in pituitary macroadenomas: quantitative assessment with diffusion tensor imaging early and long-term results. World Neurosurg. 2018;112:e691-e701.

19. Lima Rebouças, SC, Crivello, F, Tsuchida, A, et al. Association of retinal nerve layers thickness and brain imaging in healthy young subjects from the i-Share-Bordeaux study. HUM BRAIN MAPP. 2023; 44 (13): 4722-4737.

20. Ito, Y, Sasaki, M, Takahashi, H, et al. Quantitative Assessment of the Retina Using OCT and Associations with Cognitive Function. OPHTHALMOLOGY. 2020; 127 OPHTHALMOLOGY. doi: 10.1016/j.ophtha.2019.05.021.

21. Lee G, Park K, Oh SY, Kong D. Analysis of Optic Chiasmal Compression Caused by Brain Tumors Using Optical Coherence Tomography Angiography. Scientific Reports. 2020; 10: 2088.

22. Cennamo G, Solari D, Montorio D, et al. Early vascular modifications after endoscopic endonasal pituitary surgery: The role of OCT-angiography.PLoS ONE. 2020; 15: e0241295.

23. Ben Ghezala I, Haddad D, Blanc J, et al. Peripapillary Microvascularization Analysis Using Swept-Source Optical Coherence Tomography Angiography in Optic Chiasmal Compression. Journal of Ophthalmology. 2021; 1–9.

24. Y. Jia, J. M. Simonett, J. Wang et al., "Wide-field OCT angiography investigation of the relationship between radial peripapillary capillary plexus density and nerve fiber layer thickness," Investigative Opthalmology & Visual Science,vol. 58, no. 12, pp. 5188–5194, 2017.

25. de Blank, P, Fisher, MJ, Gittleman, H, et al. Validation of an automated tractography method for the optic radiations as a biomarker of visual acuity in neurofibromatosis-associated optic pathway glioma. EXP NEUROL. 2017; 299 (Pt B): 308-316.

26. Kwapong, WR, Peng, C, He, Z, et al. Altered Macular Microvasculature in Neuromyelitis Optica Spectrum Disorders. AM J OPHTHALMOL. 2018; 192 47-55.

27. Wang, G, Gao, J, Yu, W, et al. Changes of Peripapillary Region Perfusion in Patients with Chiasmal Compression Caused by Sellar Region Mass. J OPHTHALMOL. 2021; 2021 5588077.

28. Wang, X, Chou, Y, Zhu, H, et al. Retinal Microvascular Alterations Detected by Optical Coherence Tomography Angiography in Nonfunctioning Pituitary Adenomas. Transl Vis Sci Technol. 2022; 11 (1): 5.

Tables

Table 1
General data comparison between the case and control groups.

	PA group (N = 24)	Control group (N = 24)	χ^2/t	P
Gender				
Male	15	12	0.75	0.05
Female	9	12		
Age (year)	47.958 ± 15.638	50.291 ± 16.619	-0.501	0.619
BCVA (LogMAR)	0.150 ± 0.314	0.041 ± 0.064	2.335	0.022*
MD (dB)	1.295 ± 2.586	0.191 ± 0.349	2.931	0.004*

Table 2
Comparative analysis of DTI parameters within the visual pathway for both the case and control groups.

FA value and ADC value ($\times 10^{-9}mm^2/s$)	Case group (48 eyes)	Control groups (48 eyes)	t	P
Optic nerve	0.536 ± 0.080	0.569 ± 0.066	-2.163	0.033*
	1.457 ± 0.378	1.247 ± 0.283	3.085	0.003*
Optic chiasma	0.312 ± 0.083	0.384 ± 0.061	-3.387	0.001*
	1.552 ± 0.421	1.663 ± 0.284	-1.077	0.288
Optic tract	0.448 ± 0.055	0.481 ± 0.063	-2.685	0.009*
	1.418 ± 0.169	1.423 ± 0.231	-0.125	0.901
Optic radiation	0.557 ± 0.057	0.594 ± 0.050	-3.255	0.002*
	0.887 ± 0.091	0.856 ± 0.077	2.252	0.027*

Table 3
Differential assessment of retinal OCTA parameters between the case and control groups.

OCTA parameters of macular region and optic disc	Case group (48 eyes)	Control group(48 eyes)	t	*P*
Macular DCP	23.789 ± 4.085	25.315 ± 3.532	-1.981	0.051
Video disc DCP	10.256 ± 3.328	10.963 ± 4.303	-0.900	0.371
Macular DVC	26.506 ± 4.635	28.409 ± 3.980	-2.184	0.031*
Video disc DVC	12.995 ± 3.583	13.938 ± 4.439	-1.145	0.255
Macular ICP	22.092 ± 3.772	23.875 ± 2.752	-2.680	0.009*
Video disc ICP	15.005 ± 3.626	15.788 ± 4.355	-0.957	0.341
Macular SVC	22.276 ± 6.660	25.761 ± 5.105	-2.915	0.004*
Video disc SVC	33.288 ± 6.110	36.619 ± 7.146	-2.455	0.016*
Macular SVP	28.448 ± 5.911	32.763 ± 4.523	-4.068	0.000*
Video disc SVP	20.116 ± 2.924	21.615 ± 5.096	-1.767	0.080
Video disc RPCP	35.088 ± 6.374	39.257 ± 6.600	-3.148	0.002*

Table 4
Comparative assessment of OCT parameters between the case and control groups.

OCT parameter (um)	Case group (24 cases, 48 eyes)	Control group (24 cases, 48 eyes)	t	P
Average CP-RNFL	107.750 ± 9.619	113.270 ± 8.943	-2.912	0.004*
Nasal CP-RNFL	79.125 ± 18.922	79.583 ± 18.363	-0.120	0.904
Supra CP-RNFL	136.395 ± 17.148	141.312 ± 17.675	-1.383	0.170
Temporal CP-RNFL	76.437 ± 14.352	85.437 ± 16.892	-2.813	0.006*
Inferior CP-RNFL	139.125 ± 13.878	147.437 ± 15.923	-2.726	0.008*
Macular GCL, IPL, and GCC thickness				
Nasal inner ring	46.791 ± 5.656	49.166 ± 6.223	-1.956	0.053
	39.875 ± 3.699	41.270 ± 3.740	-1.838	0.069
	106.125 ± 10.188	124.104 ± 14.189	-5.941	0.000*
Supra inner ring	49.854 ± 6.010	52.125 ± 4.290	-2.130	0.036*
	40.125 ± 3.330	41.791 ± 3.786	-2.290	0.024*
	113.750 ± 11.092	117.791 ± 8.644	-1.991	0.049*
Temporal inner ring	44.854 ± 6.052	46.125 ± 6.183	-1.017	0.312
	39.687 ± 3.477	39.854 ± 4.390	-0.206	0.837
	101.520 ± 8.975	102.229 ± 10.431	-0.357	0.722
Inferior inner ring	47.812 ± 8.509	50.333 ± 7.438	-1.545	0.126
	38.666 ± 5.423	40.125 ± 4.270	-1.464	0.147
	109.520 ± 17.079	113.229 ± 14.286	-1.154	0.251

Table 5
Analysis highlighting correlations among OCTA parameters, OCT parameters, and visual pathway DTI parameters.

Correlation coefficient	Macular DCP	Macular DVC	Macular ICP	Macular SVC	Macular SVP	Macular DCP	Para-optic disk DVC	Para-optic disk SVC	optic disk RPCP
ADC value of optic nerve									
r	-0.235	-0.228	-0.210	-0.207	-0.478	-0.129	0.021	0.068	0.039
P	0.268	0.284	0.325	0.331	0.018*	0.549	0.923	0.753	0.856
FA value of optic tract									
r	0.287	0.208	0.182	0.267	0.557	0.054	-0.073	-0.160	-0.114
P	0.174	0.330	0.395	0.206	0.005*	0.803	0.736	0.454	0.594
FA value of optic radiation									
r	0.502	0.552	0.516	0.472	0.568	0.599	0.462	0.101	0.160
P	0.012*	0.005*	0.010*	0.020*	0.004*	0.002*	0.023*	0.637	0.456
ADC value of optic emission									
r	-0.505	-0.529	-0.548	-0.617	-0.640	-0.111	-0.043	-0.499	-0.526
P	0.012*	0.008*	0.006*	0.001*	0.001*	0.606	0.842	0.013*	0.008*
Inner ring below RNFL thickness									
r	0.215	0.158	0.113	0.503	0.544	/	/	/	/
P	0.324	0.460	0.598	0.012*	0.006*	/	/	/	/
GCL thickness below inner ring									
r	0.195	0.183	0.130	0.597	0.656	/	/	/	/
P	0.362	0.392	0.545	0.002*	0.001*	/	/	/	/
IPL thickness below inner ring									

| Correlation coefficient	Macular DCP	Macular DVC	Macular ICP	Macular SVC	Macular SVP	Macular DCP	Para-optic disk DVC	Para-optic disk SVC	optic disk RPCP
r	0.155	0.106	0.049	0.475	0.549	/	/	/	/
P	0.459	0.621	0.820	0.019*	0.005*	/	/	/	/
Top CP-RNFL									
r	/	/	/	/	/	0.050	0.123	0.383	0.505
P	/	/	/	/	/	0.816	0.567	0.064	0.012*
Temporal CP-RNFL									
r	/	/	/	/	/	0.334	0.292	0.301	0.408
P	/	/	/	/	/	0.111	0.166	0.153	0.048*
Below CP-RNFL									
r	/	/	/	/	/	0.265	0.182	0.563	0.642
P	/	/	/	/	/	0.211	0.396	0.004*	0.001*
Average CP-RNFL									
r	/	/	/	/	/	0.381	0.401	0.471	0.626
P	/	/	/	/	/	0.066	0.052	0.020*	0.001*

Figures
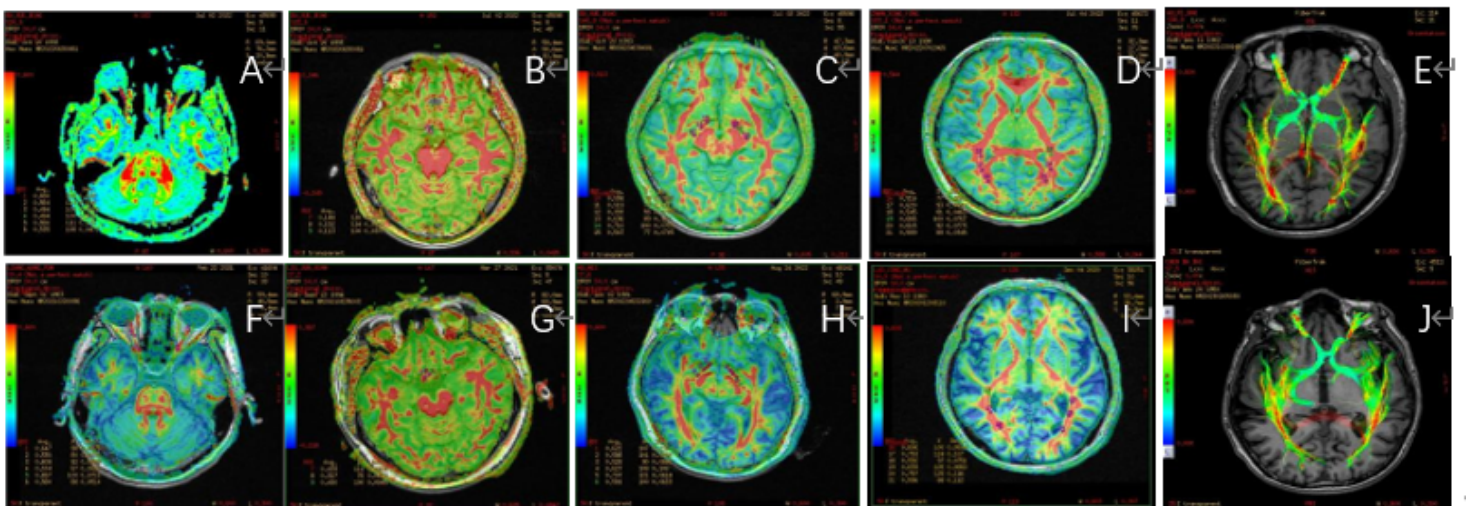
Figure 1

Images of FA reveal the disparities between the case group, denoted as A-E, and the control group, labeled as F-J. Measurements derived from seed points are shown at the bottom right of each image. Specific regions depicted include: A/F: Optic nerve; B/G: Optic chiasm; C/H: Optic chiasm; D/I: Optic tract; E/J: Visual pathway.
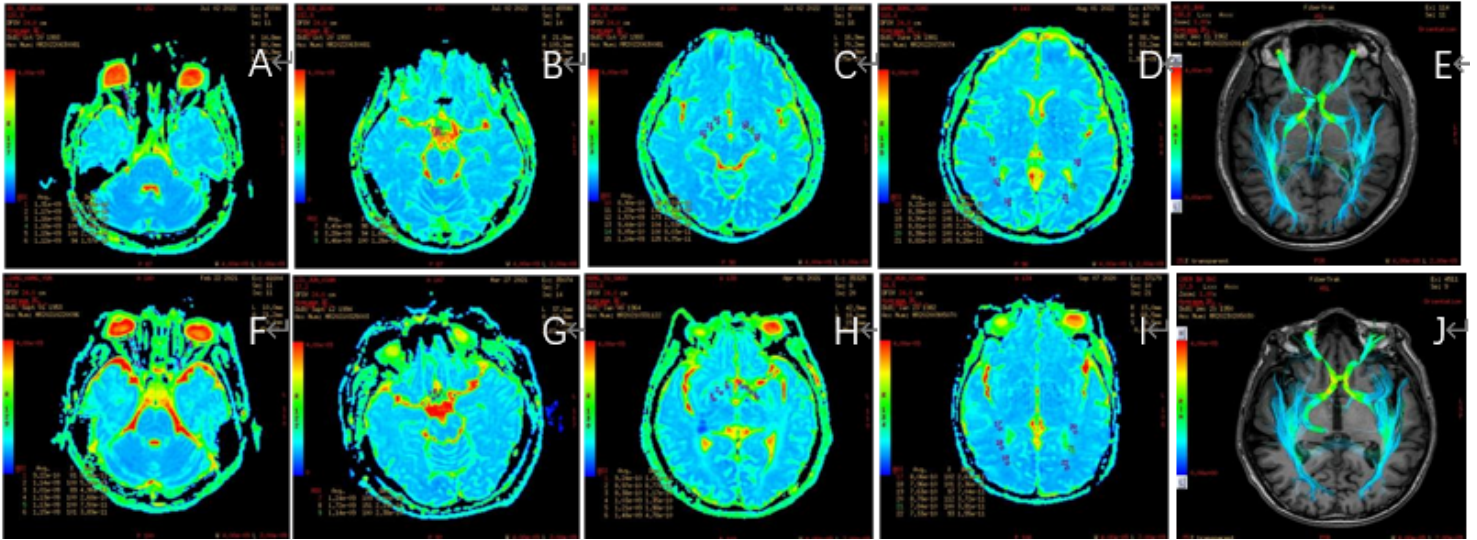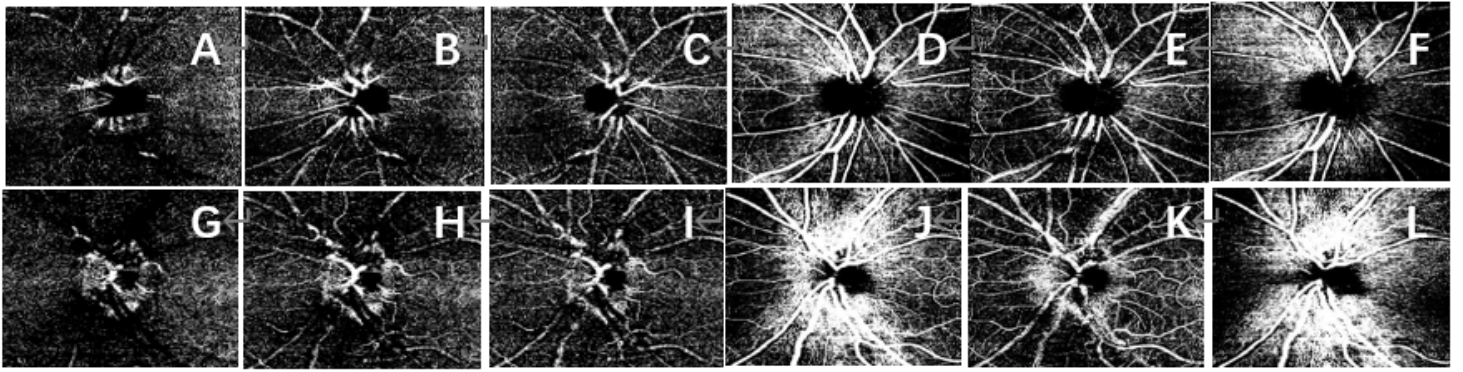

Figure 2

ADC images showcasing variations between the case group (A-E) and the control group (F-J). Measurements from seed points are positioned at the bottom right. Regions included are: A/F: Optic nerve; B/G: Optic chiasm; C/H: Optic chiasm; D/I: Optic tract; E/J: Visual pathway.
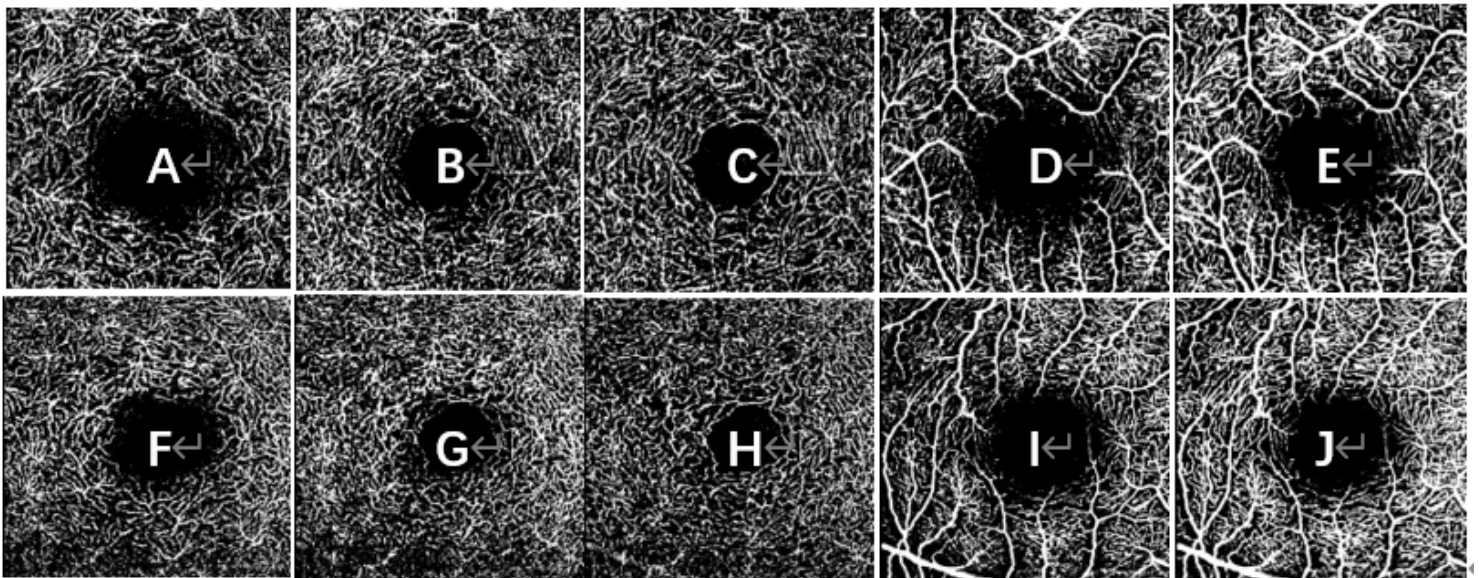
Figure 3

Binarized OCTA images detailing blood flow density in various macular region layers for the case (A-E) and control (F-G) groups. Layers displayed include: A/F: DCP; B/G: DVC; C/H: ICP; D/I: SVC; E/G: SVP.

Figure 4

Binarized OCTA images presenting blood flow density in layers of the optic disc region for the case (A-F) and control (G-L) groups. Layers represented are: A/G: DCP; B/H: DVC; C/I: ICP; D/J: SVC; E/K: SVP; F/L: RPCP.